Revista Brasileira de Ensino de Física, vol. 46, e20240063 (2024)
www.scielo.br/rbef
DOI: https://doi.org/10.1590/1806-9126-RBEF-2024-0063

Didactic Resources

Electromechanical energy conversion between a DC motor and a capacitor bank: a compreensive and low-cost experiment

Gustavo Salustiano[1], Ivan Guilhon[*1], Tiago Admiral[2]

[1]Instituto Tecnológico de Aeronáutica, Laboratório de Pesquisa em Educação Científica e Tecnológica, São José dos Campos, SP, Brasil.
[2]Instituto Federal de Educação, Ciência e Tecnologia Fluminense, Campos dos Goytacazes, RJ, Brasil.

Received on February 21, 2024. Accepted on July 03, 2024.

In this work, we present an experiment that illustrates an electromechanical energy conversion between a DC motor and electrolytic capacitors. The DC motor is coupled to a rigid disk and initially powered by a voltage supply, then the power supply is disconnected, and the electrical machine is connected to an electric diode in series with a capacitor bank. The stored charge in the capacitor bank demonstrates that the device, previously working as a DC motor, starts operating as an electric generator. The proposed experiment can be used to discuss the physical model of DC motor, induced electromotive forces, diode characteristic curve, and dynamics of the capacitors. We present a comprehensive mathematical model for the capacitor charging dynamics and characterize the relevant circuit parameters. Computational simulations are performed and predicted final capacitor voltages and electromechanical conversion efficiencies are compared with the experimental data. The overall agreement between the proposed model and experimental data is very good.
Keywords: Electric circuits, motors, electromechanical conversion.

1. Introduction

Electromechanical energy conversion systems are used in wind, hydroelectric, thermal, and thermonuclear power plants, as well as several home appliances and vehicles. The possibility of efficient generation of electric power and the invention of direct and alternate current (DC and AC, respectively) electric motors changed the way of life of humankind in XX century [1].

A comprehension of involved physical phenomena related to these systems – mainly magnetic forces on wires crossed by electric currents and electromagnetic induction [2] is necessary, not only for physics students and engineers, but for the whole society. Beyond the basic physical principles related to electric machines, students should understand an electric generator or an electric motor could be realistically modeled by the combination of power supplies, resistors, inductors, and other circuit elements usually presented in expository instructions.

It is well known that the same electric machine can, in principle, function as an electric generator or an electric motor, depending on the application circumstances. This versatility in energy conversion may not be evident to inexperienced students [3]. Thus, a combination of explanatory discourse and hands-on experimentation is welcome to clarify this important aspect.

The use of models can assist us in teaching how the physical properties of a system influence the dynamics of variations of a specific parameter in a circuit [4]. Simultaneously, simulations within the model can provide, within a short timeframe, the same values obtained by numerical methods, involving appropriate software, or even conventional spreadsheets [5].

In this work we present a low-cost electromechanical system based on DC electric motor. In the proposed experiment, we highlight how the DC can be converted in an electric generator, which is a non-conventional application of this device. We varied relevant parameters and performed different measurements to explore the relationship between these quantities and justify the circuit model of the DC motor. To explicit this behavior, we use the DC motor in electric generator mode to charge electric capacitors. Electric diodes are used to allow electric current only in the charging direction.

In a didactic context, it is interesting to highlight that this experiment can be used to integrate knowledge about different involved electromagnetic phenomena, such as the DC motor circuit model, the operation of electric diodes, and the dynamics of a capacitor charging process. Therefore, it can offer fruitful discussions that go beyond simple qualitative demonstrations.

*Correspondence email address: guilhon@ita.br

This is an innovative and interesting didactic experiment which can be used both with both high school and undergraduates, depending on the level of discussions. The used materials are cheap and measurements can be done with conventional power supplies and multimeters. We investigate the angular speed of the DC motors both with an Arduino board [6–8] and video acquisition with Tracker software [9]. The proposed experimental method also explores computational tools as Python numerical and scientific libraries, such as Numpy and Scipy [10–12].

This work is organized as follows. In section 2 we present relevant concepts of the modeling of DC motors and diodes, as well as the mathematical modelling of charging dynamics. The relevant parameters are presented, as well how the proposed circuit is assembled. In section 3, we present the experimental set-up and how the measurements were made. In section 4, we present and discuss the obtained results, comparing them with our theoretical model whenever possible. Finally, in section 5 we provide a summary and conclusions.

2. Theoretical Background

2.1. Electric motor theoretical model

Electrical machines are devices that allow energy conversion between electrical and mechanical forms. When the device converts mechanical energy to mechanical energy, it works as a generator; while when it converts electrical energy to mechanical energy, it works as a motor. It is worthy to mention that a given electric device can work converting energy in both ways according to given circumstances [1].

The wide availability of electric energy, its low associated costs and ease of control contributed to its widespread use both in houses and industry. Among a myriad of technological applications of electric motors, one can cite fans, blenders, washing machines, air compressors in refrigerator systems, elevators, and electric cars. That are several kinds of electric motors, which might be powered with AC or DC electric currents [1]. In this work, we focus our discussion to the modelling of simple versions of 6V DC electric motors. These motors are commonly found in electric toys powered by batteries.

A simple DC motor is made of a stator, a rotor, a commutator, and brushes. The stator is stationary in the motor and contains the magnets that provide the magnetic field responsible for the magnetic flux in the rotor. The rotor is the moving component, containing the windings of wires that allow current to flow. The flowing current in the magnetic field generates a torque in the rotor, via Lorentz force, which makes it spin.

As previously said, such a device can also be used as an electric generator. If the motor axis is connected to a source of mechanical energy that exerts a net torque over it, the rotation of the rotor generates a potential difference via Faraday's law, allowing the generation of electric currents in a load circuit.

DC motors can be modelled by equivalent circuits composed of idealized electric components [1]. Since this electric device is based on great lengths of wires winded in coils, we consider an internal resistance r associated with the wire resistance. This resistance decreases the motor's efficiency, since part of the power is dissipated in the form of heat due to Joule's law and drop of voltage given by Ohm's law

$$U_d = ri. \tag{1}$$

The intense winding of the coil generates a self-inductance L_m. This parameter limits the motor's time response to establish a steady current in a given operation condition. In cases when the applied voltage rapidly changes, the self-inductance may be associated with a characteristic transition time. The reactive voltage associated with this parameter is given by the equation

$$U_{rec} = L_m \frac{di}{dt}. \tag{2}$$

When an electric machine works – whether motor or generator – the magnetic flux through its coils varies according to its angular velocity and an electromotive force is induced. When the machine works as an electric generator, the voltage is the generator electric force that powers the load. On the other hand, when the electric machine works as a motor, the induced voltage is characterized as a back electromotive force.

The exact instant value may exhibit fast oscillations according to the electric motor geometry and angular velocity ω. Assuming, for example, a simple closed wire of area A rotating with an angular velocity ω in a uniform magnetic field B, Faraday's law allows calculating the induced voltage

$$\mathcal{E}_m(\theta) = -\frac{d(BAcos\theta)}{dt} = BAsin\theta\,\omega. \tag{3}$$

The mean voltage $\mathcal{E}_m$ given by equation 3 considering a 2π rad cycle would be zero, however many DC motors (i) uses a brush scheme to invert the polarization of induced voltage and (ii) explore more sophisticated magnets and winding geometries to obtain a signal with lower ripple amplitudes.

Despite its possible fast oscillations, the mean induced voltage is expected to be linear regarding the angular velocity ω as given by the equation

$$\mathcal{E}_m = k_e\omega, \tag{4}$$

where k_e is a proportionality constant the needs to by experimentally determined. The considered equivalent series circuit model for DC motors is shown in Fig. 1.

Finally, the proposed model of our DC model, must include mechanical losses. After initial experimental

 DOI: https://doi.org/10.1590/1806-9126-RBEF-2024-0063

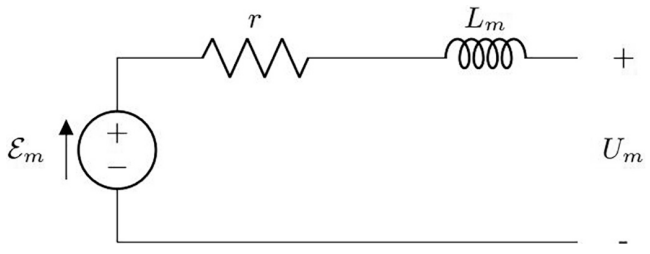

Figure 1: Equivalent circuit of a DC motor.

trials, we decided to model the friction torque on motor axis as two components

$$\tau_d = -c_0 - c_1\omega, \tag{5}$$

where the first term represents dry friction and the second an effective 'viscous' friction. Since $\tau_d = I\frac{d\omega}{dt}$ and neglecting any other source of power dissipation, one observed the following time equation for the motor's angular velocity

$$\frac{d\omega}{dt} = -\alpha_0 - \alpha_1\omega, \tag{6}$$

while $\omega(t) > 0$. The Eq. 6 can be directly integrated resulting into

$$\omega(t) = \frac{(\alpha_0 + \alpha_1\omega_0)e^{-bt} - \alpha_0}{\alpha_1}. \tag{7}$$

2.2. Diode model

A diode is an electrical component which only allows current to flow in a specific direction when a sufficient voltage is applied. In the circuit proposed by this paper, its role is to block any current flow from the charged capacitor back to the electric generator when the disk rotation ceases. This preventing its discharge and allow the register of the maximum voltage produced between the capacitor terminal along the discharge process.

A reasonably realistic diode can be modelled with the following exponential equation

$$i = i_0\left[\exp\left(\frac{eV}{nk_BT}\right) - 1\right], \tag{8}$$

where i is the current flowing through the diode, V is the voltage applied to it, I_0 is the saturation current, e is the elementary charge, k_B is the Boltzmann constant, T is the temperature and n is a non-ideality factor, ranging from 1 to 2. For an ideal diode, n is equal to 1. However, in real diodes, n is typically greater than 1 due to factors such as recombination and non-idealities in the diode structure. At room temperature, $\frac{kT}{e} = 25\ mV$ is a valid approximation [13].

The diode model can be simplified for low voltages. Its I-V characteristic is approximated by a horizontal and a vertical line. If the voltage is smaller than a specific forward voltage V_F, the diode prevents any electric current flow. If the V_F forward voltage is achieved, the diode lets the current pass in its forward direction, exhibiting an approximately constant voltage between its terminals. For diodes made of silicon, the typical V_F is around 0.7 V, while for diodes made of germanium, it is approximately 0.3 V [13]. A comparison between the exponential and simplified models is shown in Fig. 2

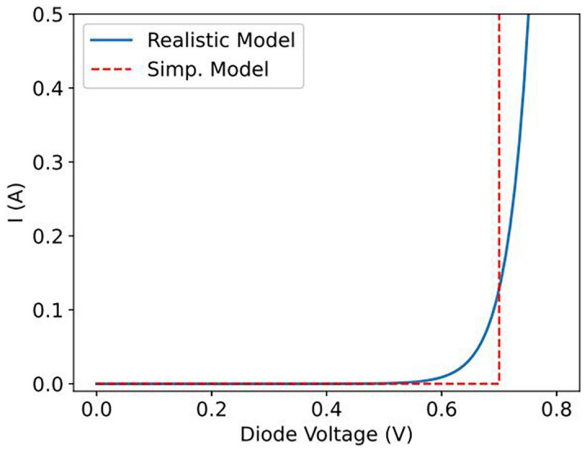

Figure 2: Diode I-V characteristic curves according to a conventional exponential model with $I_0 = 1$ nA and $n = 1.5$ (Realistic model) and the adopted simplified model for silicon diodes, assuming V_F= 0.7 V.

The proposed model does not cover any behavior that can be exhibited by electric diodes, such as the inverse leakage or breakdown currents, that might occur when reverse applied voltages are applied. For our application, typical leakage currents of a few nA are negligible and any applied voltage is not enough to promote significant reverse currents.

2.3. Circuit diagram and its modes of operation

The experimental arrangement aimed to replicate the circuit shown in Figure 3. When placed in position A, the motor is powered by an external voltage source $\mathcal{E}$, causing it to reach its final speed for that voltage. After charging the DC motor with the voltage source, it rotates with a constant angular speed. This initial phase is of great importance to the experiment since it sets the initial condition for our system.

When the switch shown in Fig. 3 is placed in position B, the motor M starts working as an electric generator, producing an electric current that flows through the diode and charges the capacitor C. The diode serves the purpose of ensuring that electric current does not flow back into the motor, thereby guaranteeing the charging of the capacitors.

When the motor is connected to the circuit with the capacitor, its charging can be modelled using kirchhoff's law

$$\mathcal{E}_m = U_d + U_{rec} + V_F + U_c, \tag{9}$$

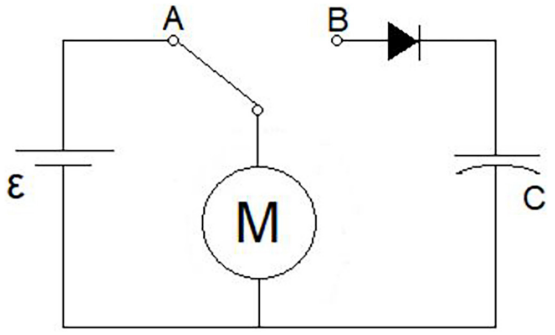

Figure 3: Basic diagram of the experimental setup.

where U_c is voltage between the terminals of the capacitor and can be easily measured after the motor stops. It can be written in terms of the stored electric charge as

$$U_c = \frac{Q}{C}. \tag{10}$$

Thus, the equation 9 can be rewritten as

$$k_e\omega = ri + L_m\frac{di}{dt} + V_F + \frac{Q}{C}. \tag{11}$$

The dynamic state of our system will be characterized my the triple $v = [\omega, i, Q]^T$. The equation 11 stands for a first dynamical equation of the system.

A second relationship between state variables may be obtained by including an electric dissipation term in Eq. 6, due to the loss of energy of the motor to the rest of the circuit, given by

$$\frac{d\omega}{dt} = -\alpha_0 - \alpha_1\omega - \alpha_2 i, \tag{12}$$

where α_2 is a braking coefficient associated with the dissipation of energy via Joule's effect. Its value can be estimated by equaling the mechanical power $\tau\omega$ with the one electric power $\mathcal{E}_m i$. Letting I be the total moment of inertia moment of the rotor and mechanical loads attached to it, one writes $\tau = I\frac{d\omega}{dt}$, where τ is an effective torque due to the electric dissipation. Thus,

$$I\frac{d\omega}{dt}\omega = k_e\omega i \rightarrow \frac{d\omega}{dt} = \frac{k_e}{I}i. \tag{13}$$

Therefore, we estimate the α_2 coefficient as

$$\alpha_2 = \frac{k_e}{I}. \tag{14}$$

Then, we remember the relationship between electric current i and stored charge Q, which works as our third dynamical equation:

$$i = \frac{dQ}{dt}. \tag{15}$$

Finally, the system dynamics may be summarized in a matrix form as

$$\frac{d}{dt}\begin{bmatrix}\omega\\ i\\ Q\end{bmatrix} = \begin{bmatrix}-\alpha_1 & -\alpha_2 & 0\\ \frac{k_e}{L_m} & -\frac{r}{L_m} & -\frac{1}{L_m C}\\ 0 & 1 & 0\end{bmatrix}\begin{bmatrix}\omega\\ i\\ Q\end{bmatrix} + \begin{bmatrix}-\alpha_0\\ V_F\\ 0\end{bmatrix}, \tag{16}$$

which can be simulated with an appropriate ordinary differential equation integrator until $i > 0$. After this instant, the charging process is completed ($i = 0$ A and Q remains constant) and the electric machine stops due to the mechanical friction in a few seconds.

The quality of the proposed model can be evaluated by comparing the predicted final capacitor voltage U_c with its experimental values.

3. Experimental Procedure

The metallic disc, coupled to the motor shaft, was used to ensure greater reliability in the value of the moment of inertia. Since the moment of inertia of the internal motor structures was neglected, it was necessary to have a measurable parameter I to perform theoretical estimates.

The DC motor was secured on a wooden support. At the base of this support, there are three screws used for aligning the assembly. Attached to the motor's shaft is a metal disk with a radius of $R = (14.85 \pm 0.05)$ cm and a mass of $M = (507.8 \pm 0.1)$ g, giving the system a moment of inertia of $I = (5.6 \pm 0.4).10^{-3}$ kg.m^2. In a more detailed manner, the actual experimental arrangement can be observed in Figure 4.

In Figure 4, two voltmeters (V_1 and V_2) can also be observed. V_1 was employed to measure the voltage supplied by the external source ($\mathcal{E}$), even though it includes a voltage indication, this value does not provide high precision. A voltmeter V_2 was utilized to measure the voltage at the terminal of the capacitor assembly at the conclusion of the charging process.

The Arduino was also employed in the setup, along with a lap counter sensor; its purpose was to measure the angular velocity $\omega(t)$ of the disk. Regarding the

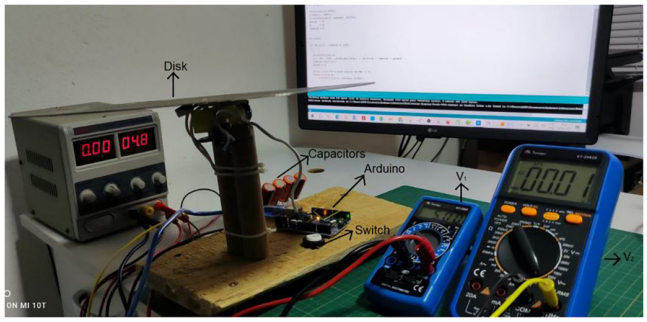

Figure 4: Image of the actual experimental setup, with certain components highlighted.

 DOI: https://doi.org/10.1590/1806-9126-RBEF-2024-0063

measurement of angular velocity, the sensor used essentially operated as a logical pulse counter. Positioned just beneath the disk, a small decoder with a known number of holes caused the light to be interrupted a certain number of times per second, and the Arduino loaded with the following scheme provided the value of angular velocity. The source code used is provided in Appendix A.

In order to model the behavior of the circuit and the equations governing it, it was necessary to gather more details about the function $\omega(t)$. To achieve this, videos of the disk's motion were recorded, and analysis was conducted using the Tracker software [9].

Two techniques were required for measuring ω because, although the use of Arduino provided us with a very precise instantaneous value of ω, the program had a limitation when it came to providing the change of the parameter over time. Therefore, the Arduino was used solely to determine the value of ω_0, while the Tracker application provided us with the values of $\omega(t)$.

The DC motor internal resistance can be measured with a conventional ohmmeter and its inductance, measured directly with an inductance meter. In addition to the measurements of r and L, another important parameter, k_e, was obtained indirectly. We vary the applied voltage $\mathcal{E}$ and measure the electric current I and angular velocity ω in the steady regime. The k_e coefficient is given by

$$k_e = \frac{\mathcal{E} - ri}{\omega} \tag{17}$$

and they are presented later in Table 1. To perform the measurements, the switch was placed in position A, and the voltage was gradually increased until reaching the desired value, which was verified on V_1. Then, the magnitude of ω_0 was read on the Arduino's serial monitor and recorded. Subsequently, we can calculate the value of k_e from Eq. 17.

The α_1 and α_2 friction parameter can be determined by the investigation of how the angular velocity $\omega(t)$ varies from an initial value after the power supply of the electric motor is disconnected. An experimental essay is performed, the experimental $\omega(t)$ is measured and compared with the behavior predicted by Eq. 7. The α_1 and α_2 parameters are estimated by the minimization of the squared error.

As the electromotive force provided by the motor is known to be limited to small values, the amount of stored energy would depend on the total capacitance value of the assembly. To achieve a large capacitance, we use a set of five parallel-connected electrolytic capacitors (each with $6800\mu F/35V$) with an equivalent capacitance of 31.94 mF, charging the assembly.

At the end of the motion, the voltage value at the terminal of the assembly was displayed on V_2, and the value was recorded as well. At the conclusion of each measurement, the capacitor terminals were shorted for complete discharge before starting another measurement.

4. Results and Discussion

4.1. Determination of the DC motor parameters

We start the experiment characterizing the physical parameters of the DC motor. The DC motor used has a nominal voltage of $6.0V$. The motor internal resistance and self-inductance can be directly measured by an ohmmeter and an inductance meter, respectively. The obtained results were

$$r = 3.4 \pm 0.4\,\Omega \tag{18}$$

and

$$L_m = 0.901 \pm 0.001\,mH. \tag{19}$$

Five supply voltages V_s are applied to the motor and the correspondent disk's angular velocities ω_o are measured 20 times to estimate statistical uncertainties. The average electric current required to maintain the motor at its speed ω_o and the voltage between its terminals, U_m, were also measured using a conventional multimeter. The obtained results and respective uncertainties are reported in Table 1.

Applying the Eq. 17 for the five operation points, we estimate the parameter

$$k_e = 0.216 \pm 0.005\,V.s/rad. \tag{20}$$

The braking coefficient α_2 is then given by Eq. 14. For our experimental set-up we obtain

$$\alpha_2 = 38.5\ \text{rad.A}^{-1}.\text{s}^2. \tag{21}$$

To estimate the α_0 e α_1 friction parameters, we apply a voltage of 5.0 V to the DC motor connected to the disk load. The angular velocity $\omega(t)$ is measured as a function of time and displayed in Fig. 5. The collected experimental data is compared with the simplified expected behavior expressed by Eq. 6. The friction parameters determined by the minimization of squared error are given by

$$\alpha_0 = 2.76 \pm 0.25\,\text{rad.s}^{-2} \tag{22}$$

Table 1: Mean ω_o ($\pm 0.1 rad/s$) and $\mathcal{E}$ ($\pm 0.01V$) values for each applied motor voltage. Errors associated with the measurements of the current i_o are all within the range of $\pm 0.001A$.

$\mathcal{E}$ [V]	ω_o [rad/s]	i [A]
4.00	16.3	0.122
4.50	18.8	0.125
5.00	21.4	0.128
5.50	24.3	0.132
6.00	26.1	0.135

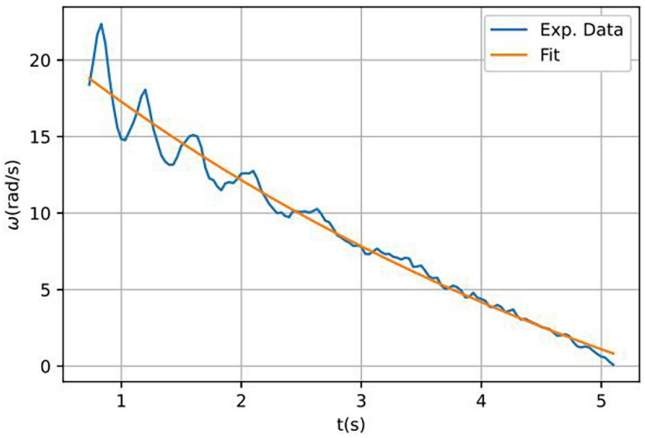

Figure 5: Measurements of disk's angular velocity as a function of time (blue curve). The predicted values by the combination of dry and viscous frictions are given by the orange curve. This result was obtained using a source voltage of 5.0 V.

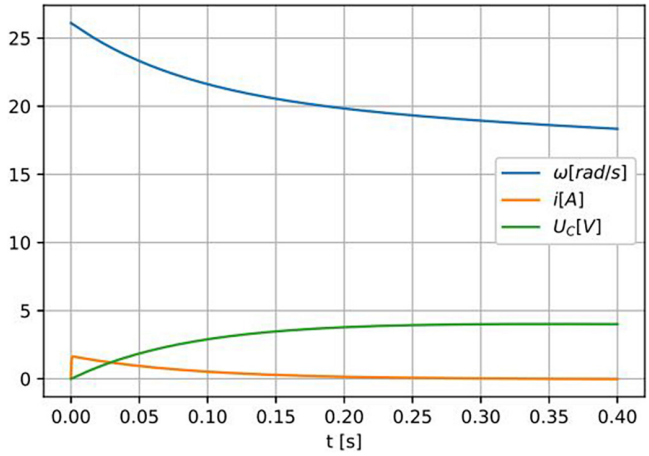

Figure 6: Simulation results of the theoretical model for the initial conditions associates with $\mathcal{E}$= 6.00 V, ω_0= 26.1 rad/s, and $i_0 = 0.135$ A. The blue, green, and orange curves represent the behavior of the angular velocity $\omega(t)$ of the disk in rad/s, the electric current $i(t)$ in A, electric voltage $U_C(t)$ between the terminals of the capacitor, respectively.

and

$$\alpha_1 = 0.170 \pm 0.027\,\mathrm{s}^{-1}. \tag{23}$$

The non-predicted observed oscillations might be associated with the model simplifications, such as the finite number of poles in the electric machine, and set-up mechanical oscillations neglected by our model. However, the overall agreement is satisfactory.

4.2. Capacitor charging process

Each operation point listed in Table 1 corresponds to a different initial condition for the charging process. The evolution of the circuit state is then ruled by Eq. 16, until the voltage between the electric generator is not large enough to establish a forward electric current. Figure 6 shows the evolution of ω, i, and U_C until the voltage between capacitor terminals becomes stable for the initial source voltage on the DC motor of $\mathcal{E}$= 6.00 V. Other initial conditions results in similar behaviors.

One observed that the charging time of the capacitor is very short, about 0.33 s for the considered initial conditions. Therefore, the capacitor charge is almost instantaneous for the considered values. However, this might not be true for larger $\tau_C = rC$ charging time constants.

In Table 2, we provide a comparison between theoretical predictions of the final voltage between capacitor terminals, U_C, and experimental data collected in our experiments, $U_{C,Exp}$. One observes that the theoretical predictions exhibit an overall qualitative agreement with the measured results, with some results being within experimental estimated uncertainties. The theoretical values exhibit larger results, which might be associated with losses not considered by our theoretical model and the simplification of the electric diode.

No significant variation of charging time is observed for the different initial conditions. The fact that the capacitor charging is completed after about 0.33 s, according to the performed simulations, after the switch is connected to point B in Fig. 3, while the disk stills holds a significant angular velocity, limits the energy conversion efficiency. From the Table 2, it becomes clear that the efficiency of transfer is roughly constant, slight varying around the mean value of 14.1%.

Table 2: Comparison between experimental and theoretical final capacitor voltages ($U_{C,Exp}$ and U_C, respectively), simulated charging times Δt, and experimental energy conversion efficiencies η for different supply voltages $\mathcal{E}$. The values of η are given by the ratio between the experimental final stored energy in the capacitor and the initial mechanical energy.

$\mathcal{E}$ [V]	$U_{C,Exp}$ [V]	U_C [V]	Δt [s]	η_{Exp} [%]
4.00	2.36 ± 0.04	2.51	0.32	14.2
4.50	2.80 ± 0.10	2.91	0.32	15.1
5.00	3.00 ± 0.10	3.33	0.33	13.3
5.50	3.50 ± 0.10	3.80	0.33	14.1
6.00	3.70 ± 0.20	4.09	0.34	13.6

The low value of efficiency can be explained by three reasons: small charging time constants, mechanical losses due to friction and electrical dissipation in diode polarization and internal resistances. In general, we observed larger energy conversion efficiencies for larger capacitance values. A calculated energy balance estimated through the performed computer simulations is provided in Tab. 3.

During the capacitor charge, the electric losses ($E_R + E_D$) and mechanical losses (E_m) are comparable. One observes that the energy dissipated in diode, E_d, is more relevant for smaller source voltages, varying from 4.8% to 7.5% for the considered initial conditions. The substitution of a conventional silicon diode by one made of germanium, with smaller forward voltages V_F, should result in smaller polarization losses. The variation of

 DOI: https://doi.org/10.1590/1806-9126-RBEF-2024-0063

Table 3: The electromechanical efficiency predicted by our simulations and dissipated energies fractions among different sources: internal electric resistance (E_R), diode polarization (E_D), friction during capacitor charge (E_m) and friction after capacitor charge (E'_m).

$\mathcal{E}$ [V]	η_{Teo}[%]	E_R [%]	E_D [%]	E_m [%]	E'_m [%]
4.00	13.5	10.0	7.5	15.6	53.3
4.50	13.7	10.0	6.6	14.8	54.9
5.00	13.8	10.0	5.8	14.1	56.2
5.50	13.9	10.1	5.1	13.5	57.3
6.00	14.0	10.1	4.8	13.2	57.9

the fraction of energy dissipated in DC motor internal resistance, E_R, only exhibits slight variations about 10 % during the charging processes.

Our calculations indicate mechanical losses associated to friction after the charging is completed, E'_m, is responsible for the dissipation of more than half of the initial energy of the system in all cases, which indicates that the electromechanical conversion efficiency is enhanced for larger capacitance values. This modification implies larger charging times and the consequent decrease of E'_m.

Finally, one observes an agreement between predicted and experimental electromechanical efficiencies within an average discrepancy of 0.64%, which stands as a second indicator of the quality of the proposed model for the system.

5. Summary and Conclusions

In this work, we propose an experiment that explores the possibility of switching between the motor and electric generator of a same electrical machine, usually presented as simply 'DC motor'. The electromechanical energy conversion is presented from a power source to the DC motor, and then from the electric generator – priorly working as a motor – to an electric capacitor.

A theoretical background focusing on the modelling of the different electric compounds is presented, specially concerning the electric model of a DC motor and its braking coefficients.

All the relevant physical parameters are experimentally measured, and computational simulations based on the proposed dynamic equations are performed. The predicted values of final capacitor voltage U_C are compared with the actually measured ones, exhibiting a good agreement and showing the quality of the proposed theoretical model for the system. For the considered initial conditions, electromechanical efficiencies of about 14% were measured and calculated, also with very good agreement.

The physical principles involved in this experiment are accessible to a broad range of students, ranging from elementary to undergraduates. Of course, the mathematical modeling of capacitor charging, as well the exercise of computational simulations, would be restricted to college students. Some of their results and insights, however, can be discussed with younger students. In particular, we explore the energy balance of the system and discuss some modification that could result in larger efficiencies.

This is a creative and cheap solution that can support general science, physics, and engineering teaching. The use of different auxiliary technologies such as microcontrollers, video tracking and computer simulations was adopted to provide open-source tools that allow the student to quantitatively investigate the phenomenon.

Acknowledgements

The authors thank Laboratório de Pesquisa em Educação Científica e Tecnológica (LPECT), Instituto Tecnológico de Aeronáutica, and Núcleo de Pesquisa em Física e Ensino de Ciências (NPFEC), for infrastructure and support.

A. Arduino Source Code Used in the Angular Velocity Measurements

In this appendix, we provide the source code for angular velocity measurements made by Arduino. This code provides an RPM measurement of a rotating disk, leveraging interrupts for accurate pulse counting. The calculated RPM is displayed on the serial monitor.

In the code, we can observe the initial declaration of variables. The variable "pperlap," which is assigned the value of 20, represents the number of holes in the decoder. This will signal the program that upon receiving 20 pulses from a specific moment onward, it signifies a complete revolution of the disc. Subsequently, the update rates for the serial monitor (set at 115200) and the input pin that will monitor the pulses are declared.

Subsequently, the function "$attachInterrupt''$ associates the function "$counter''$ with the interrupt of pin 2 with a detection of rising pulses. Within the "loop" function, the operation assigned to "w'' calculates the rotations per minute based on the pulses detected over a $1.0s$ interval. The information is then displayed on the serial monitor, and the pulse count is reset with the action "$pulses = 0''$.

Listing 1: Arduino source code made to measure the disk angular velocity.

```
int             w;
volatile byte pulses;
unsigned long timeold;
unsigned int pperlap = 20;
void counter ()
{
    pulses++;
}
void setup()
{
  Serial.begin(115200);
  pinMode(2, INPUT);
```

```
  attachInterrupt(0, counter, RISING);
  pulses  = 0;
  w       = 0;
  timeold = 0;
  }
void loop()
{
  if (millis() - timeold >= 1000)
  {
 detachInterrupt(0);
 w=(60*1000/pperlap)/(millis()-timeold)
 *pulses;
 timeold = millis();
 pulses = 0;
 Serial.print("RPM:");
 Serial.println(w);
 attachInterrupt(0, counter, RISING);
  }
}
```

References

[1] S.J. Chapman, *Electric Machinery Fundamentals* (McGraw-Hill, New York, 2011), 5 ed.

[2] A.J. Richards, The Physics Teachers **58**, 572 (2020).

[3] P.C. Hecking, The Physics Teachers **45**, 445 (2007).

[4] C. Xuan, The Physics Teachers **61**, 503 (2023).

[5] D.T. Young, The Physics Teachers **61**, 31 (2023).

[6] Arduino, available in: http://arduino.cc/.

[7] A.A. Galadima, in: *2014 11th International Conference on Electronics, Computer and Computation (ICECCO)* (Abuja, 2014).

[8] G. Organtini, Journal of Physics: Conference Series **1076**, 012026 (2018).

[9] D. Brown and A.J. Cox, The Physics Teacher **47**, 145 (2009).

[10] G. Van Rossum, *Python reference manual*, available in: https://ir.cwi.nl/pub/5008/05008D.pdf.

[11] P. Virtanen, R. Gommers, T.E. Oliphant, M. Haberland, T. Reddy, D. Cournapeau, E. Burovski, P. Peterson, W. Weckesser, J. Bright et al., Nature Methods **17** 261 (2020).

[12] C.R. Harris, K.J. Millman, S.J. van der Walt, R. Gommers, P. Virtanen, D. Cournapeau, E. Wieser, J. Taylor, S. Berg, N.J. Smith et al., Nature **585**, 357 (2020).

[13] A.S. Sedra and K.C. Smith, *Microelectronic Circuits* (Oxford University Press, Oxford, 2004).